

Reproducing kernel enhanced local radial basis collocation method

J. S. Chen^{1,*},[†], W. Hu¹ and H. Y. Hu²

¹*Civil & Environmental Engineering Department, University of California, Los Angeles (UCLA), CA, U.S.A.*

²*Mathematics Department, Tunghai University, Taiwan, Republic of China*

SUMMARY

Standard radial basis functions (RBFs) offer exponential convergence, however, the method is suffered from the large condition numbers due to their ‘nonlocal’ approximation. The nonlocality of RBFs also limits their applications to small-scale problems. The reproducing kernel functions, on the other hand, provide polynomial reproducibility in a ‘local’ approximation, and the corresponding discrete systems exhibit relatively small condition numbers. Nonetheless, reproducing kernel functions produce only algebraic convergence. This work intends to combine the advantages of RBFs and reproducing kernel functions to yield a local approximation that is better conditioned than that of the RBFs, while at the same time offers a higher rate of convergence than that of reproducing kernel functions. Further, the locality in the proposed approximation allows its application to large-scale problems. Error analysis of the proposed method is also provided. Numerical examples are given to demonstrate the improved conditioning and accuracy of the proposed method. Copyright © 2007 John Wiley & Sons, Ltd.

Received 24 August 2007; Revised 6 November 2007; Accepted 7 November 2007

KEY WORDS: reproducing kernel; local radial basis function; collocation method

1. INTRODUCTION

Radial basis function (RBF) was originally constructed for interpolation [1], and the multiquadrics RBF was shown to be related to the solution of the biharmonic potential problem and thus has a physical foundation [2]. RBF performs very well in interpolating highly irregular scattered data compared with many interpolation methods [3], and it has been introduced in high-dimensional

*Correspondence to: J. S. Chen, Civil & Environmental Engineering Department, University of California, Los Angeles (UCLA), CA, U.S.A.

[†]E-mail: jschen@seas.ucla.edu

Contract/grant sponsor: Lawrence Livermore National Laboratory (USA)

Contract/grant sponsor: National Science Council (Taiwan, Republic of China)

interpolation in neural networks [4]. The work by Buhmann and Micchelli [5] showed that RBFs are prewavelets (wavelets without orthogonality properties), and certain RBFs are effective projectors in multiresolution analysis, particularly when the data structure is scattered [6]. RBF was first applied to solving partial differential equations (PDEs) in [7, 8], and the theoretical foundation of the RBF method for solving PDEs has been well studied [9, 10]. Applications of RBF for solving PDEs include, for example, singularity problems [11], Hamilton–Jacobi equations [12], fourth-order elliptic and parabolic problems [13], approximation in boundary element method for nonlinear elliptic PDEs [14], hyperbolic conservation laws [15], and by employment of smoothed multilevel approach [16]. The RBF collocation method is shown to be more effective if boundary conditions are properly weighted [17].

If the approximated function and the RBFs satisfy certain regularity conditions, RBFs exhibit exponential convergence in interpolation [18, 19]. However, while enjoying the exponential convergence, the RBF collocation method yields a full discrete system and consequently ill-conditioned as the discrete dimension increases. This leads to a convergence problem in addition to the high CPU in dealing with a full matrix, and it constitutes the major bottleneck in applying RBF to large-scale computation. The shape parameter of RBF greatly influences the linear dependency and consequently the condition number of the discrete system as reported in [20]. Several attempts have been made to resolve this difficulty. The block partitioning method takes the advantage of better conditioning of each sub-block [21]. The multizone method was applied to transient problem where the transient solution of each smaller nonoverlapping zone is better conditioned [22]. An adaptive algorithm [23] has been proposed to properly select suitable new test and trial spaces iteratively. Alternatively, the ill-conditioning of the RBF collocation method has been enhanced by introducing a compactly support RBF truncated from polynomials that are strictly positive definite [24]. However, reasonable accuracy of these truncated functions can be achieved only when sufficiently large support is employed.

In contrast to the global approximation in RBF collocation method based on strong form, mesh-free local approximations have been introduced in solving PDEs based on weak form and Galerkin approximation, for example, moving least-squares (MLS) approximation [25, 26], reproducing kernel (RK) approximation [27, 28], and partition of unity [29, 30]. In these methods, the locality and smoothness of the approximation are defined in the kernel function with compact support, and basis functions are introduced either intrinsically or extrinsically to the kernel function to achieve certain order of completeness or to embed certain characteristic functions of the PDEs in the approximation. A dilemma in the mesh-free method based on Galerkin weak form is the need to perform domain integration. Introducing collocation method to the weak form yields spatial instability, while the Gauss integration consumes considerable CPU. A compromised approach is to introduce a stabilization to the nodally integrated weak form [31, 32]. Imposition of Dirichlet boundary conditions is another time-consuming process in the Galerkin-based mesh-free methods [33, 34]. Although the employment of MLS or RK approximations yields algebraic convergence regardless of the locality of the approximation, these methods with localized approximation yield very well conditioned discrete equations, and the solution remains stable as the discretization is refined.

In this work, we introduce a combined RK and RBF approximation to achieve a local approximation that has the similar convergence property as that of the RBF collocation method while yielding a banded and better-conditioned discrete system. The essential idea is to correct RBF with a compactly supported kernel function that reproduces polynomials. Localizing RBF with polynomial reproducibility yields a convergence between RBF exponential convergence and RK

algebraic convergence. Several numerical examples are analyzed to examine the performance of the proposed method.

This paper is organized as follows. In Section 2, the fundamental properties of RBFs are reviewed. In Section 3, the basic equations of RK approximation are introduced, the construction of RK-enriched RBF is presented, and the convergence properties are discussed. The implementation of localized RBF with collocation method for solving boundary value problems is given in Section 4. Numerical examples demonstrating the effectiveness of the proposed method are presented in Section 5. Conclusion remarks are given in Section 6.

2. RADIAL BASIS FUNCTIONS

Let $\Omega \subset R^d$, $d \geq 1$, be a closed region with boundary $\partial\Omega$, and let \mathbf{S} be a set of N_s source points,

$$\mathbf{S} = [\mathbf{x}_1, \mathbf{x}_2, \dots, \mathbf{x}_{N_s}] \subseteq \Omega \cup \partial\Omega \quad (1)$$

For a smooth function $u(\mathbf{x})$, the approximation, denoted by $v(\mathbf{x})$, is expressed as

$$v(\mathbf{x}) = \sum_{I=1}^{N_s} g_I(\mathbf{x}) a_I + p(\mathbf{x}) \quad (2)$$

where a_I is the expansion coefficient, $p(\mathbf{x}) \in P_t$ is a polynomial of degree less than t on R^d , and $g_I(\mathbf{x})$ is the RBF, for example, the multiquadrics (MQ) RBF:

$$g_I(\mathbf{x}) = (r_I^2 + c^2)^{n-3/2}, \quad n = 1, 2, 3, \dots \quad (3)$$

where $r_I = \|\mathbf{x} - \mathbf{x}_I\|$, and the constant c involved in Equation (3) is called the *shape parameter* of RBF. The convergence of RBF has been studied by Madych [35], and it has been shown that there exists an exponential convergence rate if RBF is globally analytic or band limited

$$|u(\mathbf{x}) - v(\mathbf{x})| \approx O(\eta^{c/h}) \quad (4)$$

where $0 < \eta < 1$, $\eta = \exp(-\theta)$ with $\theta > 0$, and h is the radial distance defined as

$$h := h(\Omega, \mathbf{S}) = \sup_{\mathbf{x} \in \Omega} \min_{\mathbf{x}_I \in \mathbf{S}} \|\mathbf{x} - \mathbf{x}_I\| \quad (5)$$

Accuracy and rate of convergence of MQ-RBF approximation are determined by the number of basis functions (the number of source points) N_s and the shape parameter c . The use of variable shape parameters may enhance the accuracy, see Kansa and Hon [21].

The exponential convergence of RBF, however, is overshadowed by its ‘global’ (nonlocal) approximation in solving PDEs, and it yields a full matrix in discrete equations. Further, under the collocation framework in solving PDEs, the condition number of matrices in the discrete equations increases significantly as the number of source points increases. It has been shown [36] that RBF is capable of reproducing constant and linear functions in *infinite* domain. However, RBF cannot reproduce constant and linear functions in *finite* domain with finite number of source points:

$$\sum_{I=1}^N (\alpha + \beta x_I) g_I(x) \neq (\alpha + \beta x) \quad (6)$$

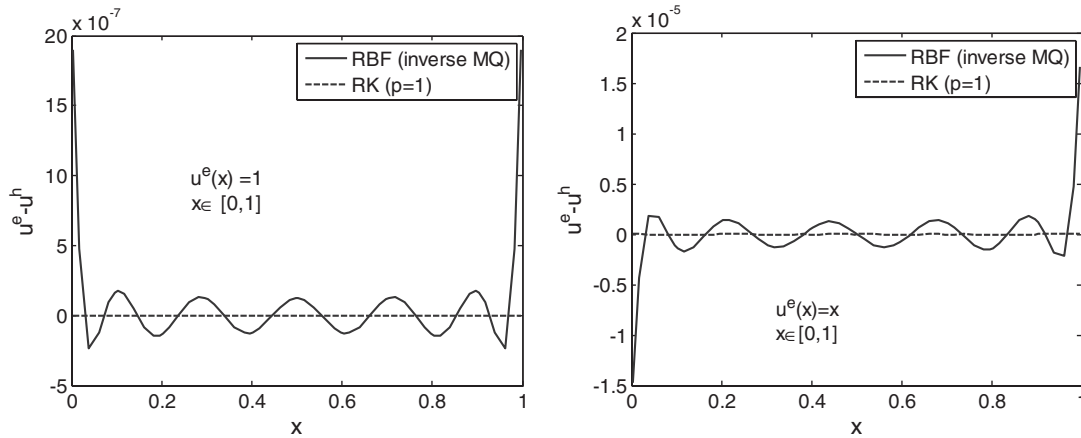


Figure 1. Errors in the reproduction of one-dimensional constant and linear polynomial functions by RBF and RK function.

On the other hand, some local approximation methods such as RK approximation [27, 28] are constructed to reproduce polynomials for random point distributions in the finite domain. As shown in Figure 1, RBF exhibits errors in reproducing constant and linear functions in a finite domain [0, 1], whereas RK function with linear basis ($p=1$) yields exact reproduction of constant and linear functions using 11 random points.

Recall RBF given in Equation (2) and let $W^{k,p}(\Omega) = \{w | D^\alpha w \in L^p(\Omega), |\alpha| \leq k\}$ be the Sobolev space, where D^α denotes the α th-order partial derivative operator. If the function u is sufficiently smooth, $u \in W^{k,2}(\Omega) \cap L^p(\Omega)$, $k > \frac{1}{2}$, $p \in [2, \infty)$, Madych and Nelson [19] based on the earlier work by Golomb and Weinberger [37] showed the following algebraic convergence:

$$\|v - u\|_{L^p(\Omega)} \leq ch^{k-d/2+d/p} \|u\|_{W^{k,2}(\Omega)} \tag{7}$$

If further restrictive conditions on the approximated function u and the RBF g_I are considered as follows:

$$\int_{\mathbb{R}^d} \frac{|\tilde{u}(\xi)|^2}{\tilde{g}_I(\xi)} d\xi < \infty \tag{8}$$

$$\int_{\mathbb{R}^d} \|v\|^l \tilde{g}_I(\xi) d\xi \leq \rho^l l! \quad \forall l \geq 2k \tag{9}$$

where $\tilde{u}(\xi)$ and $\tilde{g}_I(\xi)$ are Fourier transformations of $u(x)$ and $g_I(x)$, respectively, ρ is a positive number, then the following exponential convergence result has been shown by Madych and Nelson [18]

$$\|v - u\|_{L^\infty(\Omega)} \leq C\eta^{c/h} \|u\|_t \tag{10}$$

where C is a constant independent of c and h , $0 < \eta < 1$ is a real number, and $\|\cdot\|_l$ is induced from conditions (8) and (9) [18]. The numerical examples given in Hu *et al.* [11] and Cheng *et al.* [38] verified the above exponential convergence.

3. LOCALIZED RBF APPROXIMATION

3.1. Localization of RBF by reproducing kernel

Let \mathbf{T} be a set of N_p points in $\bar{\Omega} = \Omega \cup \partial\Omega$

$$\mathbf{T} = \{\mathbf{x}_1, \mathbf{x}_2, \dots, \mathbf{x}_{N_p}\}, \quad \mathbf{x}_I \in \bar{\Omega}, \quad I = 1, 2, \dots, N_p \quad (11)$$

The set is used to define a finite open covering $C = \{\omega_I\}_{I=1}^{N_p}$ of Ω , where $\Omega \subset \bigcup_{I=1}^{N_p} \omega_I$ as shown in Figure 2, and the covering $C = \{\omega_I\}_{I=1}^{N_p}$ of Ω satisfies an overlapping condition

$$\exists \kappa \in N \quad \forall \mathbf{x} \in \Omega \quad \text{card}\{I | \mathbf{x} \in \omega_I\} \leq \kappa \quad (12)$$

A class of functions $\{\phi_I(\mathbf{x})\}_{I=1}^{N_p}$ is called a partition of unity subordinated to the open covering C if it possesses the following property:

$$\sum_{I=1}^{N_p} \phi_I(\mathbf{x}) = 1 \quad \forall \mathbf{x} \in \Omega \quad (13)$$

The partition of unity function can be constructed by

$$\phi_I(\mathbf{x}) = \varphi_a(\mathbf{x} - \mathbf{x}_I) b(\mathbf{x}) \quad (14)$$

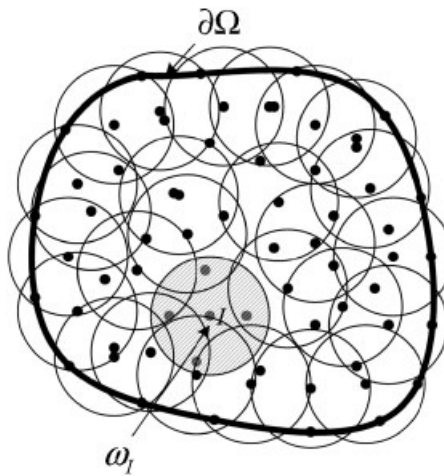


Figure 2. Discretization of domain by finite covers.

where $\varphi_a(\mathbf{x}-\mathbf{x}_I)$ is a kernel function defined on the finite cover ω_I centered at \mathbf{x}_I , and a is the radius of the finite cover ω_I . Usually, $\varphi_a(\mathbf{x}-\mathbf{x}_I)>0$ for $\mathbf{x}\in\omega_I$ is selected. Here, $b(\mathbf{x})$ is a function to be thought to meet partition of unity condition

$$\sum_{I=1}^{N_p} \phi_I(\mathbf{x}) = \left(\sum_{J=1}^{N_p} \varphi_a(\mathbf{x}-\mathbf{x}_J) \right) b(\mathbf{x}) = 1 \tag{15}$$

By obtaining $b(\mathbf{x}) = 1 / \sum_{J=1}^{N_p} \varphi_a(\mathbf{x}-\mathbf{x}_J)$, we have

$$\phi_I(\mathbf{x}) = \frac{\varphi_a(\mathbf{x}-\mathbf{x}_I)}{\sum_{J=1}^{N_p} \varphi_a(\mathbf{x}-\mathbf{x}_J)} \tag{16}$$

The partition of unity function in Equation (13) is the Shepard function. To achieve higher-order approximation, a reproducing kernel (RK) function by modification of Equation (14) has been proposed [28]

$$\phi_I(\mathbf{x}) = \varphi_a(\mathbf{x}-\mathbf{x}_I) \left[\sum_{|\alpha| \leq p} (\mathbf{x}-\mathbf{x}_I)^\alpha b_\alpha(\mathbf{x}) \right] \tag{17}$$

Here, we use the multi-dimensional notation $\alpha = (\alpha_1, \dots, \alpha_d)$ with $d > 1$ the integers representing the dimension. The quantity $|\alpha| = \sum_{i=1}^d \alpha_i$ is the length of α , $\mathbf{x}^\alpha = x_1^{\alpha_1}, \dots, x_d^{\alpha_d}$, $\{(\mathbf{x}-\mathbf{x}_I)^\alpha\}_{|\alpha| \leq p}$ is a set of monomial basis functions with degree less than or equal to p , and $b_\alpha(\mathbf{x}) = b_{\alpha_1, \dots, \alpha_d}(\mathbf{x})$, $|\alpha| \leq p$, are the coefficients of the basis functions that vary with the location of approximation \mathbf{x} . Coefficients $b_\alpha(\mathbf{x})$ are determined from the following reproducing conditions:

$$\sum_I \phi_I(\mathbf{x}) \mathbf{x}_I^\alpha = \mathbf{x}^\alpha, \quad |\alpha| \leq p \tag{18}$$

Equation (18) is equivalent to

$$\sum_I \phi_I(\mathbf{x}) (\mathbf{x}-\mathbf{x}_I)^\alpha = \delta_{|\alpha|,0}, \quad |\alpha| \leq p \tag{19}$$

or

$$\sum_I \phi_I(\mathbf{x}) \mathbf{H}(\mathbf{x}-\mathbf{x}_I) = \mathbf{H}(\mathbf{0}) \tag{20}$$

$$\begin{aligned} \mathbf{H}^T(\mathbf{x}-\mathbf{x}_I) &= [(\mathbf{x}-\mathbf{x}_I)^\alpha]_{|\alpha| \leq p} \\ &= [1, x_1 - x_{1I}, \dots, x_d - x_{dI}, (x_1 - x_{1I})^2, \dots, (x_d - x_{dI})^p] \end{aligned} \tag{21}$$

Substituting Equation (17) into Equation (18) to obtain $b_\alpha(\mathbf{x})$, and the RK function $\phi_I(\mathbf{x})$ into Equation (17) reads

$$\phi_I(\mathbf{x}) = \mathbf{H}^T(\mathbf{0}) \mathbf{M}^{-1}(\mathbf{x}) \mathbf{H}(\mathbf{x}-\mathbf{x}_I) \varphi_a(\mathbf{x}-\mathbf{x}_I) \tag{22}$$

where

$$\mathbf{M}(\mathbf{x}) = \sum_I \mathbf{H}(\mathbf{x} - \mathbf{x}_I) \mathbf{H}^T(\mathbf{x} - \mathbf{x}_I) \varphi_a(\mathbf{x} - \mathbf{x}_I) \quad (23)$$

The function $\phi_I(\mathbf{x})$ is called the RK shape function. Conditions assuring the nonsingularity of the matrix $\mathbf{M}(\mathbf{x})$ as well as good performance of the method are discussed in [39], where rigorous convergence analysis and error estimates of the method are also provided.

The concept of partition of unity approximation [29, 30] is introduced herein to localize RBF with monomial reproducibility:

$$u^h(\mathbf{x}) = \sum_{I=1}^N [\phi_I(\mathbf{x})(a_I + g_I(\mathbf{x})d_I)] \quad (24)$$

where we assume $N_p = N_s = N$. In general, different RBFs or other basis functions can be employed in the approximation (24) to yield:

$$u^h(\mathbf{x}) = \sum_{I=1}^N \left[\phi_I(\mathbf{x}) \left(a_I + \sum_{J=1}^M g_I^J(\mathbf{x}) d_I^J \right) \right] \quad (25)$$

where $\phi_I(\mathbf{x})$ is the RK function, $g_I^J(\mathbf{x})$ denotes RBFs or other basis functions, for example, the multiquadrics RBF defined in (3) and a_I and d_I^J are the corresponding coefficients.

Rewrite the localized RBF approximation in Equation (25) as

$$u^h(\mathbf{x}) = \sum_{I=1}^N \phi_I(\mathbf{x}) u_I^h(\mathbf{x}) \quad (26)$$

where

$$u_I^h(\mathbf{x}) \in V_I, \quad V_I = \text{span}\{1, g_I^1, g_I^2, \dots, g_I^M\} \quad (27)$$

and

$$u^h(\mathbf{x}) \in V, \quad V = \bigcup_{I=1}^N V_I \quad (28)$$

Assume that local approximation space V_I has the following property:

$$\|u - u_I^h\|_{\ell, \Omega \cap \omega_I} \leq T(c, \ell, I, N, M) \|u\|_t \quad \forall I, u_I^h \in V_I, \ell \geq 0 \quad (29)$$

where $\|\cdot\|_{\ell, \Omega \cap \omega_I}$ denotes the Sobolev norm, $T(\dots)$ is a term dependent on some parameters, and $\|\cdot\|_t$ is defined as in Section 2. Note that there exists an algebraic decay if monomial bases are chosen and that there exists an exponential decay if Fourier functions or RBFs are used within the radius of convergence a .

Consider a quasi-uniform support size distribution. By using the condition of partition of unity, $\sum_{I=1}^N \phi_I = 1$, and thus $\sum_{I=1}^N \phi_I(u - u_I^h) = u - \sum_{I=1}^N \phi_I u_I^h$, there exists a global

estimate [29]

$$\begin{aligned}
 \|u - u^h\|_{0,\Omega}^2 &= \left\| \sum_{I=1}^N \phi_I(u - u_I^h) \right\|_{0,\Omega}^2 = \int_{\Omega} \left| \sum_{I=1}^N \phi_I(u - u_I^h) \right|^2 d\Omega \\
 &\leq \kappa \int_{\Omega} \sum_{I=1}^N |\phi_I(u - u_I^h)|^2 d\Omega = \kappa \int_{\Omega} \sum_{I=1}^N |\phi_I|^2 |u - u_I^h|^2 d\Omega \\
 &\leq \kappa C_{\infty}^2 \sum_{I=1}^N \int_{\Omega \cap \omega_I} |u - u_I^h|^2 d\Omega = \kappa C_{\infty}^2 \sum_{I=1}^N \|u - u_I^h\|_{0,\Omega \cap \omega_I}^2 \\
 &\leq \kappa^2 C_{\infty}^2 \max_I T^2(c, 0, I, N, M) \|u\|_I^2
 \end{aligned} \tag{30}$$

where κ denotes the maximal number of covers for any $\mathbf{x} \in \Omega$ defined in Equation (12), and RK shape function is bounded, that is, $|\phi_I|_{\infty} \leq C_{\infty}$. Moreover, with (29) and the exponential convergence property of (4), we have

$$\|u - u^h\|_{0,\Omega} \leq \kappa C_{\infty} \eta_0^{c/h} \|u\|_I \tag{31}$$

3.2. Inverse inequalities

The inverse inequalities of the proposed localized RBF are presented for the study of convergence and stability in the following section. Let the approximation u^h in Equation (25) be expressed as

$$v := u^h(x) = \sum_{I=1}^N \phi_I(\mathbf{x}) a_I + \sum_{I=1}^N \sum_{J=1}^M \varphi_I^J(\mathbf{x}) d_I^J =: v_1 + v_2 \tag{32}$$

where $\varphi_I^J(\mathbf{x}) = \phi_I(\mathbf{x}) g_I^J(\mathbf{x})$. We have local estimates as follows (see Appendix A for details):

$$\|v_1\|_{\ell,\omega_I}^2 \leq C_1 a^{-\ell d} p^{2\ell d} \|v_1\|_{0,\omega_I}^2 \quad \text{for } \ell \geq 1 \tag{33}$$

$$\|v_2\|_{\ell,\omega_I}^2 \leq (C_2 a^{-3\ell d/2} p^{2\ell d} + C_3 a^{-3\ell d/2} \mu^{\ell d}) \|v_2\|_{0,\omega_I}^2 \quad \text{for } \ell \geq 1 \tag{34}$$

where p is the reproducing degree, a is the maximal radius of finite cover ω_I , d is the space dimension, μ is the maximal number of RBF within cover ω_I , and C_i are generic constants. Furthermore, we obtain global estimates as follows:

$$\begin{aligned}
 \|v\|_{\ell,\Omega}^2 &= \|v_1 + v_2\|_{\ell,\Omega}^2 \leq 2\|v_1\|_{\ell,\Omega}^2 + 2\|v_2\|_{\ell,\Omega}^2 \\
 &\leq c_1 \left\{ \sum_{I=1}^N \|v_1\|_{\ell,\omega_I}^2 \right\} + c_2 \left\{ \sum_{I=1}^N \|v_2\|_{\ell,\omega_I}^2 \right\} \\
 &\leq c_3 \kappa a^{-\ell d} p^{2\ell d} \|v_1\|_{0,\Omega}^2 + (c_4 \kappa a^{-3\ell d/2} p^{2\ell d} + c_5 \kappa a^{-3\ell d/2} \mu^{\ell d}) \|v_2\|_{0,\Omega}^2
 \end{aligned} \tag{35}$$

and thus

$$\|v\|_{\ell,\Omega} \leq (c_6 \kappa^{1/2} a^{-\ell d/2} p^{\ell d} + c_7 \kappa^{1/2} a^{-3\ell d/4} p^{\ell d} + c_8 \kappa^{1/2} a^{-3\ell d/4} \mu^{\ell d/2}) \|v\|_{0,\Omega} \quad \text{for } \ell \geq 1 \quad (36)$$

where $1 < p < \kappa$, $\mu \ll N$, and c_i are generic constants.

4. WEIGHTED COLLOCATION METHOD

4.1. Strong form collocation

Consider the following general form of a boundary value problem:

$$\begin{aligned} \mathbf{L}\mathbf{u} &= \mathbf{f} \quad \text{in } \Omega \\ \mathbf{B}^h \mathbf{u} &= \mathbf{h} \quad \text{on } \partial\Omega^h \\ \mathbf{B}^g \mathbf{u} &= \mathbf{g} \quad \text{on } \partial\Omega^g \end{aligned} \quad (37)$$

where Ω is the problem domain, $\partial\Omega^h$ is the Neumann boundary, $\partial\Omega^g$ is the Dirichlet boundary, $\partial\Omega^h \cup \partial\Omega^g = \partial\Omega$, \mathbf{L} is the differential operator in Ω , \mathbf{B}^h is the differential operator on $\partial\Omega^h$, and \mathbf{B}^g is the operator on $\partial\Omega^g$.

For a multi-dimensional function \mathbf{u} , approximation \mathbf{u}^h defined at N_s source points is expressed as

$$\mathbf{u}^h = \Phi^T \mathbf{y} \quad (38)$$

where Φ is an approximation function and \mathbf{y} are the corresponding coefficients. For example, in two-dimension, we have

$$\mathbf{u}^h = \begin{bmatrix} u_1^h \\ u_2^h \end{bmatrix}, \quad \Phi^T = [\Phi_1 \quad \Phi_2 \quad \cdots \quad \Phi_{N_s}], \quad \Phi_J = \begin{bmatrix} \phi_J & 0 & \varphi_J & 0 \\ 0 & \phi_J & 0 & \varphi_J \end{bmatrix} \quad (39)$$

where $\varphi_J = \phi_J g_I$ and

$$\mathbf{y}^T = [y_1 \quad y_2 \quad \cdots \quad y_{N_s}], \quad \mathbf{y}_J^T = [a_{1J} \quad a_{2J} \quad d_{1J} \quad d_{2J}] \quad (40)$$

In standard collocation method, the residuals of Equation (37) are enforced to be zeros at the collocation points. Let \mathbf{P} be a set of N_p collocation points in Ω , \mathbf{Q} be a set of N_q collocation points on $\partial\Omega^h$, and \mathbf{R} be a set of N_r collocation points on $\partial\Omega^g$; we have

$$\mathbf{P} = [\mathbf{p}_1, \mathbf{p}_2, \dots, \mathbf{p}_{N_p}] \subseteq \Omega, \quad \mathbf{Q} = [\mathbf{q}_1, \mathbf{q}_2, \dots, \mathbf{q}_{N_q}] \subseteq \partial\Omega^h, \quad \mathbf{R} = [\mathbf{r}_1, \mathbf{r}_2, \dots, \mathbf{r}_{N_r}] \subseteq \partial\Omega^g \quad (41)$$

The source point set \mathbf{S} and the collocation point set $\mathbf{P} \cup \mathbf{Q} \cup \mathbf{R}$ may or may not have common points. By enforcing strong form of (37) to be satisfied at the collocation points, we have the following discrete equation:

$$\mathbf{A}\mathbf{y} = \mathbf{b} \quad (42)$$

where

$$\mathbf{A} = \begin{pmatrix} \mathbf{A}^1 \\ \mathbf{A}^2 \\ \mathbf{A}^3 \end{pmatrix}, \quad \mathbf{A}^1 = \begin{pmatrix} \mathbf{L}(\Phi^T(\mathbf{p}_1)) \\ \mathbf{L}(\Phi^T(\mathbf{p}_2)) \\ \vdots \\ \mathbf{L}(\Phi^T(\mathbf{p}_{N_p})) \end{pmatrix}, \quad \mathbf{A}^2 = \begin{pmatrix} \mathbf{B}^h(\Phi^T(\mathbf{q}_1)) \\ \mathbf{B}^h(\Phi^T(\mathbf{q}_2)) \\ \vdots \\ \mathbf{B}^h(\Phi^T(\mathbf{q}_{N_q})) \end{pmatrix}, \quad \mathbf{A}^3 = \begin{pmatrix} \mathbf{B}^g(\Phi^T(\mathbf{r}_1)) \\ \mathbf{B}^g(\Phi^T(\mathbf{r}_2)) \\ \vdots \\ \mathbf{B}^g(\Phi^T(\mathbf{r}_{N_r})) \end{pmatrix} \quad (43)$$

and

$$\mathbf{b} = \begin{pmatrix} \mathbf{b}^1 \\ \mathbf{b}^2 \\ \mathbf{b}^3 \end{pmatrix}, \quad \mathbf{b}^1 = \begin{pmatrix} \mathbf{f}(\mathbf{p}_1) \\ \mathbf{f}(\mathbf{p}_2) \\ \vdots \\ \mathbf{f}(\mathbf{p}_{N_p}) \end{pmatrix}, \quad \mathbf{b}^2 = \begin{pmatrix} \mathbf{h}(\mathbf{q}_1) \\ \mathbf{h}(\mathbf{q}_2) \\ \vdots \\ \mathbf{h}(\mathbf{q}_{N_q}) \end{pmatrix}, \quad \mathbf{b}^3 = \begin{pmatrix} \mathbf{g}(\mathbf{r}_1) \\ \mathbf{g}(\mathbf{r}_2) \\ \vdots \\ \mathbf{g}(\mathbf{r}_{N_r}) \end{pmatrix} \quad (44)$$

The error analysis [17] shows unbalanced errors between domain, Neumann boundary, and Dirichlet boundary terms in (42). The unbalanced errors can be better balanced if boundary collocation equations are properly weighted. Therefore, in the weighted collocation approach, the discrete equation is constructed as follows:

$$\begin{pmatrix} \mathbf{A}^1 \\ \sqrt{\alpha^h} \mathbf{A}^2 \\ \sqrt{\alpha^g} \mathbf{A}^3 \end{pmatrix} \mathbf{y} = \begin{pmatrix} \mathbf{b}^1 \\ \sqrt{\alpha^h} \mathbf{b}^2 \\ \sqrt{\alpha^g} \mathbf{b}^3 \end{pmatrix} \quad (45)$$

where α^h and α^g are weights for Neumann and Dirichlet boundary terms, respectively. In the Poisson problem, weights $\sqrt{\alpha^h} \approx O(1)$ and $\sqrt{\alpha^g} \approx O(N_s)$. In elasticity problem, $\sqrt{\alpha^h} \approx O(1)$ and $\sqrt{\alpha^g} \approx O(\max\{\lambda, \mu\}N_s)$, where λ, μ are Lamé’s constants [17].

Remarks

To achieve a better accuracy in collocation method, the number of collocation points greater than the number of source points ($N_p + N_q + N_r > N_s$) should be considered. A detailed discussion is provided in Section 4.2. Equation (42) is an overdetermined system that is typically solved by a least-squares method:

$$\mathbf{A}^T(\mathbf{A}\mathbf{y} - \mathbf{b}) = \mathbf{0} \quad (46)$$

or by a weighted least-squares method:

$$\mathbf{A}^T \mathbf{W}(\mathbf{A}\mathbf{y} - \mathbf{b}) = \mathbf{0} \quad (47)$$

where \mathbf{W} is the weight matrix. It can be shown that (47) is equivalent to the minimization of a least-squares functional with quadrature rule consistent with the collocation points.

Define a functional:

$$E(\mathbf{v}) = \frac{1}{2} \int_{\Omega} (\mathbf{L}\mathbf{v} - \mathbf{f})^2 d\Omega + \frac{1}{2} \int_{\partial\Omega^h} (\mathbf{B}^h \mathbf{v} - \mathbf{h})^2 d\Gamma + \frac{1}{2} \int_{\partial\Omega^g} (\mathbf{B}^g \mathbf{v} - \mathbf{g})^2 d\Gamma, \quad \mathbf{v} \in V \quad (48)$$

where V denotes the finite-dimensional space defined in Section 2.1. Let $\hat{E}(\cdot)$ be the discrete functional form of $E(\cdot)$:

$$\hat{E}(\mathbf{u}^h) = \min_{\mathbf{v} \in V} \hat{E}(\mathbf{v}) \quad (49)$$

and it yields the following equation:

$$\mathbf{A}^T \mathbf{W}(\mathbf{A}\mathbf{y} - \mathbf{b}) = \mathbf{0} \quad (50)$$

where \mathbf{W} is the weight matrix containing weights associated with the quadrature rules used in domain and boundary integrals of (48). Same results can be obtained for the weighted collocation method in (45) with consideration of the following functional [17]:

$$E(\mathbf{v}) = \frac{1}{2} \int_{\Omega} (\mathbf{L}\mathbf{v} - \mathbf{f})^2 d\Omega + \frac{\alpha^h}{2} \int_{\partial\Omega^h} (\mathbf{B}^h \mathbf{v} - \mathbf{h})^2 d\Gamma + \frac{\alpha^g}{2} \int_{\partial\Omega^g} (\mathbf{B}^g \mathbf{v} - \mathbf{g})^2 d\Gamma \quad (51)$$

4.2. Convergence properties

Consider an energy norm associated with (51) as

$$\|\mathbf{v}\|_E = \{\|\mathbf{L}\mathbf{v}\|_{0,\Omega}^2 + \alpha^h \|\mathbf{B}^h \mathbf{v}\|_{0,\partial\Omega^h}^2 + \alpha^g \|\mathbf{B}^g \mathbf{v}\|_{0,\partial\Omega^g}^2\}^{1/2} \quad (52)$$

We define a bilinear form $b(\cdot, \cdot)$ and a linear form $f(\cdot)$ as follows:

$$b(\mathbf{u}, \mathbf{v}) = \int_{\Omega} \mathbf{L}\mathbf{u} \cdot \mathbf{L}\mathbf{v} d\Omega + \alpha^h \int_{\partial\Omega^h} \mathbf{B}^h \mathbf{u} \cdot \mathbf{B}^h \mathbf{v} d\Gamma + \alpha^g \int_{\partial\Omega^g} \mathbf{B}^g \mathbf{u} \cdot \mathbf{B}^g \mathbf{v} d\Gamma \quad (53)$$

$$f(\mathbf{v}) = \int_{\Omega} \mathbf{f} \cdot \mathbf{L}\mathbf{v} d\Omega + \alpha^h \int_{\partial\Omega^h} \mathbf{h} \cdot \mathbf{B}^h \mathbf{v} d\Gamma + \alpha^g \int_{\partial\Omega^g} \mathbf{g} \cdot \mathbf{B}^g \mathbf{v} d\Gamma \quad (54)$$

The solution \mathbf{u}^h in (49) satisfies the following discrete equation:

$$\hat{b}(\mathbf{u}^h, \mathbf{v}) = \hat{f}(\mathbf{v}) \quad (55)$$

where $\hat{b}(\cdot, \cdot)$ and $\hat{f}(\cdot)$ are the discrete bilinear and linear forms of $b(\cdot, \cdot)$ and $f(\cdot)$, respectively. We assume that the following inequalities hold:

$$\hat{b}(\mathbf{u}, \mathbf{v}) \leq C_a \|\mathbf{u}\|_E \|\mathbf{v}\|_E, \quad \mathbf{v} \in V \quad (56)$$

$$C_b \|\mathbf{v}\|_E^2 \leq \hat{b}(\mathbf{v}, \mathbf{v}), \quad \mathbf{v} \in V \quad (57)$$

where C_a and C_b are constants. To ensure above inequalities, a crucial condition should be fulfilled

$$|\hat{b}(\mathbf{v}, \mathbf{v}) - b(\mathbf{v}, \mathbf{v})| \leq T(\hbar, a, p, \mu) = o(1) \ll 1 \quad (58)$$

where \hbar is the maximal spacing of quadrature points (collocation points), and parameters a, p, μ are defined in Section 3.2. Following the Lax–Milgram lemma, we obtain the error bound

$$\|\mathbf{u} - \mathbf{u}^h\|_E \leq \inf_{\mathbf{v} \in V} \|\mathbf{u} - \mathbf{v}\|_E \quad (59)$$

Furthermore, it can be shown that

$$\| \mathbf{u} - \mathbf{u}^h \|_E \leq c_1 \| \mathbf{L}(\mathbf{R}_N) \|_{0,\Omega} + c_2 \sqrt{\alpha^h} \| \mathbf{B}^h(\mathbf{R}_N) \|_{0,\partial\Omega^h} + c_3 \sqrt{\alpha^g} \| \mathbf{B}^g(\mathbf{R}_N) \|_{0,\partial\Omega^g} \tag{60}$$

where $\mathbf{R}_N = \mathbf{u} - \mathbf{v}$ is the remainder.

Take a two-dimensional Poisson problem as an example, following [11] and using inverse inequalities in Section 3, we obtain a bound from Equations (56) and (57):

$$| \hat{b}(v, v) - b(v, v) | \leq (c_1 \hat{h}^{q+1} a^{-(q+3)} p^{2(q+3)} + c_2 \hat{h}^{q+1} a^{-(q+3)} \mu^{q+3}) \| v \|_{1,\Omega}^2 \tag{61}$$

where q is the order of quadrature rule. We choose \hat{h} to satisfy

$$\hat{h}^{q+1} a^{-(q+3)} p^{2(q+3)} = o(1), \quad \hat{h}^{q+1} a^{-(q+3)} \mu^{q+3} = o(1) \tag{62}$$

When parameters p and μ are fixed, it follows that

$$\hat{h} = o(a^{1+2/(q+1)}) \tag{63}$$

Since $a = (p+1)h$, we have

$$\hat{h} = o(h^{1+2/(q+1)}) \tag{64}$$

This suggests that the number of collocation points should be chosen much greater than the number of source points. As such, the two-dimensional Poisson problem has the following error bound:

$$\begin{aligned} \| u - u^h \|_{\ell,\Omega}^2 &= \left\| \sum_{I=1}^N \phi_I (u - u_I^h) \right\|_{\ell,\Omega}^2 = \left\| D^\ell \sum_{I=1}^N \phi_I (u - u_I^h) \right\|_{0,\Omega}^2 \\ &\leq 2 \left\| \sum_{I=1}^N (D^\ell \phi_I) (u - u_I^h) \right\|_{0,\Omega}^2 + 2 \left\| \sum_{I=1}^N \phi_I D^\ell (u - u_I^h) \right\|_{0,\Omega}^2 \\ &\leq 2\kappa \int_{\Omega} \sum_{I=1}^N |D^\ell \phi_I|^2 |u - u_I^h|^2 d\Omega + 2\kappa \int_{\Omega} \sum_{I=1}^N |\phi_I|^2 |D^\ell (u - u_I^h)|^2 d\Omega \\ &\leq 2\kappa \int_{\Omega \cap \omega_I} \sum_{I=1}^N |D^\ell \phi_I|^2 |u - u_I^h|^2 d\Omega + 2\kappa \int_{\Omega \cap \omega_I} \sum_{I=1}^N |\phi_I|^2 |D^\ell (u - u_I^h)|^2 d\Omega \\ &\leq 2\kappa C^2 a^{-2\ell} \sum_{I=1}^N \| u - u_I^h \|_{0,\Omega \cap \omega_I}^2 + 2\kappa C_\infty^2 \sum_{I=1}^N \| u - u_I^h \|_{\ell,\Omega \cap \omega_I}^2, \quad \ell \geq 1 \end{aligned} \tag{65}$$

where $D^\ell(v)$ denotes the ℓ th-order partial derivative, and $|\phi_I|_\infty \leq C_\infty$ and $|D^\ell \phi_I|_\infty \leq C a^{-\ell}$ are used. Finally, we obtain

$$\| u - u^h \|_{\ell,\Omega} \leq C_1 \kappa \eta_\ell^{c/h} \| u \|_t + C_2 \kappa a^{-\ell} \eta_0^{c/h} \| u \|_t, \quad \ell \geq 1 \tag{66}$$

where $\| \cdot \|_t$ is induced norm defined as in Section 2.

4.3. Conditioning of discrete equation

In this section, we investigate the condition number of local RB collocation method. The discrete form of the weighted collocation method (45) can be expressed as

$$\mathbf{F}\mathbf{y}=\mathbf{r} \quad (67)$$

where

$$\mathbf{F}=\mathbf{W}^{1/2}\mathbf{A}, \quad \mathbf{r}=\mathbf{W}^{1/2}\mathbf{b} \quad (68)$$

and \mathbf{W} is associated with weights α^g and α^h in the weighted collocation method (45). The condition number of matrix \mathbf{F} is defined as

$$\text{Cond}(\mathbf{F})=\frac{\sigma_{\max}(\mathbf{F})}{\sigma_{\min}(\mathbf{F})}=\frac{\lambda_{\max}(\mathbf{F}^T\mathbf{F})^{1/2}}{\lambda_{\min}(\mathbf{F}^T\mathbf{F})^{1/2}} \quad (69)$$

where $\sigma_{\max}(\cdot)$ and $\sigma_{\min}(\cdot)$ denote the maximal and minimal singular values in the singular value decomposition for matrix \mathbf{F} , and $\lambda_{\max}(\cdot)$ and $\lambda_{\min}(\cdot)$ denote the maximal and minimal eigenvalues for matrix $\mathbf{F}^T\mathbf{F}$. Matrix $\mathbf{F}^T\mathbf{F}$ is resulting from the discrete norm $\overline{\|\cdot\|}_E$ defined as

$$\begin{aligned} \overline{\|\mathbf{v}\|}_E^2 &= \overline{\|\mathbf{L}\mathbf{v}\|}_{0,\Omega}^2 + \alpha^h \overline{\|\mathbf{B}^h\mathbf{v}\|}_{0,\partial\Omega^h}^2 + \alpha^g \overline{\|\mathbf{B}^g\mathbf{v}\|}_{0,\partial\Omega^g}^2 \\ &= \int_{\Omega} (\mathbf{L}\mathbf{v})^2 \, d\Omega + \frac{\alpha^h}{2} \int_{\partial\Omega^h} (\mathbf{B}^h\mathbf{v})^2 \, d\Gamma + \frac{\alpha^g}{2} \int_{\partial\Omega^g} (\mathbf{B}^g)^2 \, d\Gamma = \hat{b}(\mathbf{v}, \mathbf{v}) \end{aligned} \quad (70)$$

where \hat{f} denotes numerical integration. Equation (70) can be expressed in a quadratic form as

$$\overline{\|\mathbf{v}\|}_E^2 = \mathbf{y}^T \begin{bmatrix} \mathbf{F}_1^T & \mathbf{0} \\ \mathbf{0} & \mathbf{F}_2^T \end{bmatrix} \begin{bmatrix} \mathbf{F}_1 & \mathbf{0} \\ \mathbf{0} & \mathbf{F}_2 \end{bmatrix} \mathbf{y} = \mathbf{y}^T \mathbf{F}^T \mathbf{F} \mathbf{y} =: \mathbf{y}^T \mathbf{G} \mathbf{y} \quad (71)$$

where

$$\mathbf{y} = [\mathbf{a}_1, \mathbf{a}_2, \dots, \mathbf{a}_n, \mathbf{d}_1, \mathbf{d}_2, \dots, \mathbf{d}_N]^T, \quad \mathbf{G} = \mathbf{F}^T \mathbf{F} \quad (72)$$

We have the following inequalities:

$$\lambda_{\min}(\mathbf{G})\mathbf{y}^T\mathbf{y} \leq \mathbf{y}^T\mathbf{G}\mathbf{y} \leq \lambda_{\max}(\mathbf{G})\mathbf{y}^T\mathbf{y} \quad (73)$$

From Equation (58), we have

$$|\overline{\|\mathbf{v}\|}_E^2 - \|\mathbf{v}\|_E^2| = |\hat{b}(\mathbf{v}, \mathbf{v}) - b(\mathbf{v}, \mathbf{v})| \leq T(\hat{h}, a, p, \mu) \quad (74)$$

Thus,

$$\|\mathbf{v}\|_E^2 - T(\hat{h}, a, p, \mu) \leq \overline{\|\mathbf{v}\|}_E^2 \leq \|\mathbf{v}\|_E^2 + T(\hat{h}, a, p, \mu) \quad (75)$$

and

$$\lambda_{\min}(\mathbf{G}) = \min \frac{\mathbf{y}^T \mathbf{G} \mathbf{y}}{\mathbf{y}^T \mathbf{y}} \geq \min \frac{\|\mathbf{v}\|_E^2 - T(\hat{h}, a, p, \mu)}{\mathbf{y}^T \mathbf{y}} \quad (76)$$

$$\lambda_{\max}(\mathbf{G}) = \max \frac{\mathbf{y}^T \mathbf{G} \mathbf{y}}{\mathbf{y}^T \mathbf{y}} \leq \max \frac{\|v\|_E^2 + T(\hbar, a, p, \mu)}{\mathbf{y}^T \mathbf{y}} \tag{77}$$

Taking the two-dimensional Poisson problem as an example, we have estimates as follows:

$$C_1 \|v\|_{2,\Omega}^2 \leq \|v\|_E^2 - (c_1 \hbar^{q+1} a^{-(q+3)} p^{2(q+3)} + c_2 \hbar^{q+1} a^{-(q+3)} \mu^{q+3}) \|v\|_{1,\Omega}^2 \leq \overline{\|v\|_E^2} \tag{78}$$

$$\overline{\|v\|_E^2} \leq \|v\|_E^2 + (c_1 \hbar^{q+1} a^{-(q+3)} p^{2(q+3)} + c_2 \hbar^{q+1} a^{-(q+3)} \mu^{q+3}) \|v\|_{1,\Omega}^2 \leq C_2 \|v\|_{2,\Omega}^2 \tag{79}$$

The eigenvalues are bounded by

$$\lambda_{\max}(\mathbf{G}) \leq \frac{C_2 \|v\|_{2,\Omega}^2}{\mathbf{y}^T \mathbf{y}} \leq \left(c_3 \frac{\kappa a^{-2d} p^{4d}}{\mathbf{y}^T \mathbf{y}} + c_4 \frac{\kappa a^{-3d} p^{4d}}{\mathbf{y}^T \mathbf{y}} + c_5 \frac{\kappa a^{-3d} \mu^{2d}}{\mathbf{y}^T \mathbf{y}} \right) \|v\|_{0,\Omega}^2 \tag{80}$$

and

$$\lambda_{\min}(\mathbf{G}) \geq \frac{C_1 \|v\|_{2,\Omega}^2}{\mathbf{y}^T \mathbf{y}} \geq \frac{c_6 \|v\|_{0,\Omega}^2}{\mathbf{y}^T \mathbf{y}} \tag{81}$$

in which inverse inequalities in Section 3.2 are used. Consequently, the condition number is bounded by

$$\text{Cond}(\mathbf{F}) = \left(\frac{\lambda_{\max}(\mathbf{G})}{\lambda_{\min}(\mathbf{G})} \right)^{1/2} \leq \tilde{C}_1 \kappa^{1/2} a^{-d} p^{2d} + \tilde{C}_2 \kappa^{1/2} a^{-3d/2} p^{2d} + \tilde{C}_3 \kappa^{1/2} a^{-3d/2} \mu^d \tag{82}$$

Remarks

In two-dimensional case under the collocation framework, the condition number of the standard RBF is $O(N^4)$, for RK is $O(\sqrt{\kappa} a^{-2} p^4)$, and for the proposed local RBF is $O(\sqrt{\kappa} a^{-3} p^4) + O(\sqrt{\kappa} a^{-3} \mu^2)$, where $1 < p < \kappa, \mu \ll N$. Since $a = (p+1)h, h = O(1/\sqrt{N})$, and p, κ, μ are fixed in computation, we obtain the bounds in condition numbers as follows:

RBF: $\text{Cond.} \approx O(N^4) = O(h^{-8})$

RK: $\text{Cond.} \approx O(\kappa^{1/2} a^{-2} p^4) = O(h^{-2})$

proposed local RBF: $\text{Cond.} \approx O(\kappa^{1/2} a^{-3} p^4) + O(\kappa^{1/2} a^{-3} \mu^2) = O(h^{-3})$

We see that there exists a significant reduction in condition number in the proposed local RBF compared with the standard RBF.

5. NUMERICAL EXAMPLES

In the following study, MQ-RBF, Wendland function $g_{5,3}$ [24] constructed using MQ-RBF, pure RK function with quadratic basis ($p=2$) and cubic basis ($p=3$), and the proposed local RBF (L-RBF) constructed by MQ-RBF localized with RK function are compared. For RK function to converge well under collocation approach, sufficiently smooth kernel function is used. In this study, a B-spline with C^5 continuity is employed as the kernel in RK function. In all examples, the number of collocation points is selected to be four times the number of source points (discrete points), unless otherwise specified. In the following numerical analysis, we measure the solution

accuracy by computing the $L2$ norm and $H1$ norm defined as

$$\|\mathbf{u}^h - \mathbf{u}\|_0 = \left(\int_{\Omega} (u_i^h - u_i)(u_i^h - u_i) d\Omega \right)^{1/2} \tag{83}$$

$$|\mathbf{u}^h - \mathbf{u}|_1 = \left(\int_{\Omega} (u_{i,j}^h - u_{i,j})(u_{i,j}^h - u_{i,j}) d\Omega \right)^{1/2} \tag{84}$$

In the following examples, c denotes the shape parameters in RBF, h represents the nodal distance, a is the size of finite cover in the RK kernel function or Wendland function, and p is the order of polynomial bases in RK approximation.

5.1. Approximation of a sine function

A function, $\sin(2\pi x)$ for $0 \leq x \leq 1$, is approximated by the standard RBF approach, Wendland function, pure RK function, and the proposed L-RBF function. As shown in Figure 3, the local approaches such as Wendland function, RK function, and the proposed L-RBF exhibit considerably better conditioning compared with that of the standard RBF. It is observed that the condition numbers increase as discretization is refined in both standard RBF and the Wendland function with large support ($a=0.4$), whereas the condition numbers in RK, L-RBF, and Wendland function with small support are quite insensitive to the resolution of discretization. The condition numbers in L-RBF is in-between those of the standard RBF and the RK approximations. As shown in Figures 4 and 5, very poor accuracy in $L2$ and $H1$ error norms exist in the Wendland function, whereas the proposed L-RBF achieves about the same level of accuracy and convergence rates as those of the standard RBF. Further, the standard RBF solution starts to deteriorate after certain discretization refinement due to ill-conditioning, whereas the L-RBF solution yields a fairly stable convergence as the discretization is refined. Note that for Wendland function to achieve reasonable accuracy and convergence rates, very large support size ($a=0.4$) is needed. This, however, leads to ill-conditioning as discretization is refined, which is similar to that of the standard RBF.

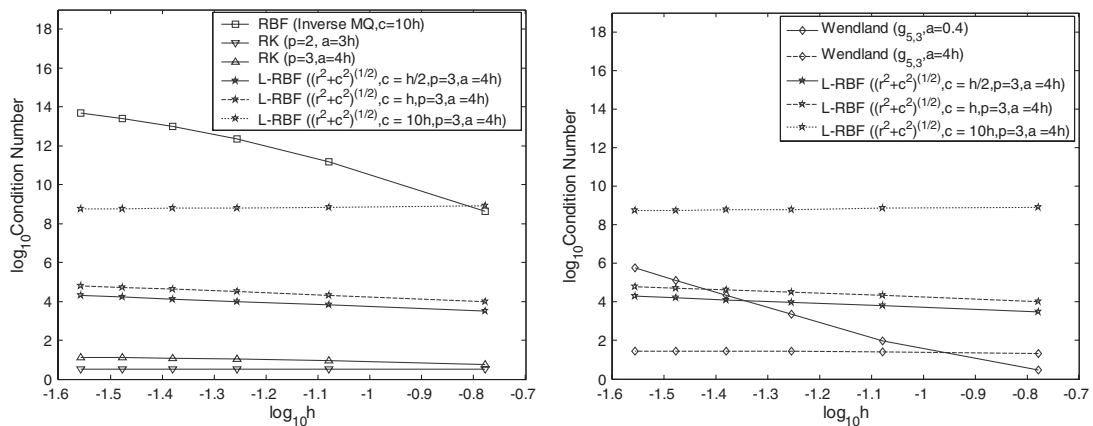


Figure 3. Condition numbers change as refinement in approximation problem.

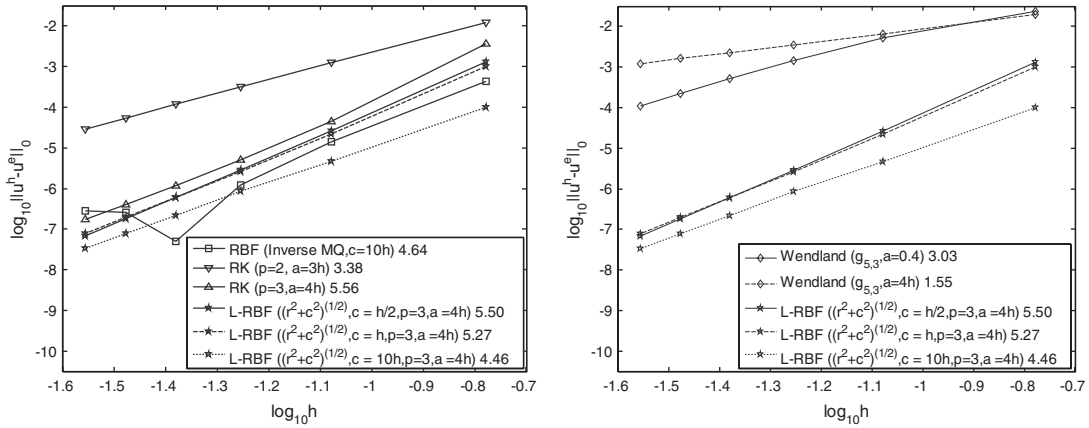


Figure 4. Convergence of \$L_2\$ error norm in approximation problem.

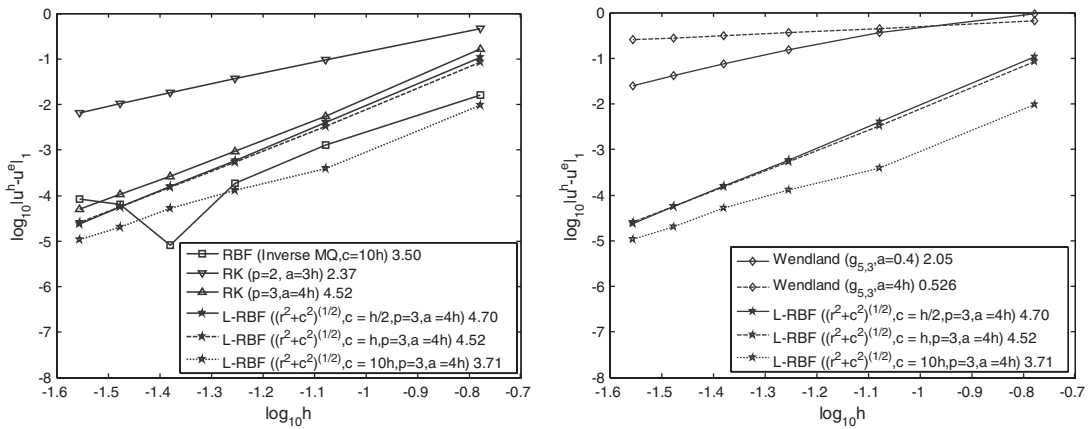


Figure 5. Convergence of \$H_1\$ error norm in approximation problem.

5.2. Two-dimensional Poisson problem

Consider the following Poisson equation:

$$\begin{aligned} \Delta u(x, y) &= (x^2 + y^2)e^{xy}, \quad \Omega = (0, 1) \times (0, 1) \\ u(x, y) &= e^{xy}, \quad \partial\Omega \end{aligned} \tag{85}$$

The condition number and convergence in \$L_2\$ and \$H_1\$ error norms are shown in Figures 6–8, respectively. The results show that L-RBF achieves a much smaller condition number compared with that of RBF and with comparable accuracy and convergence rates compared with the solution

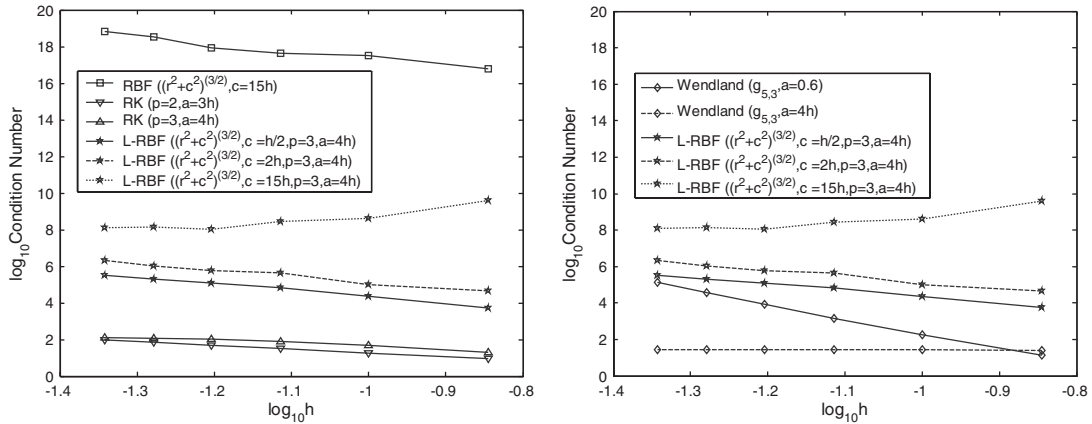


Figure 6. Condition numbers change as refinement in two-dimensional problem.

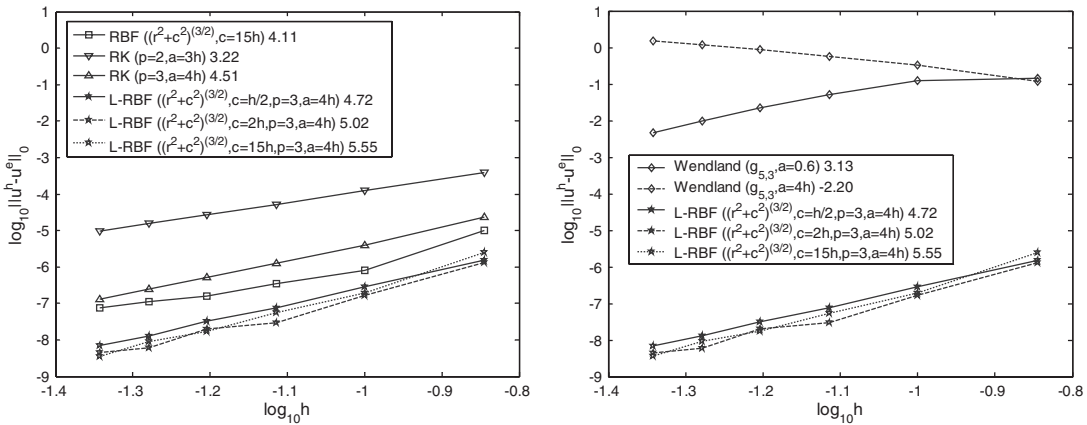


Figure 7. Convergence of L_2 error norm in two-dimensional Poisson problem.

of RBFs. Although the Wendland function also yields better conditioning compared with the RBFs, the condition number increases rapidly as the model is refined when fixed large support ($a=0.6$) is used. Further, the accuracy of Wendland function compares poorly with the proposed L-RBF. In fact, the use of small support ($a=4h$) in Wendland function does not yield a convergence in both error norms. For Wendland function to converge, a relatively large support size ($a=0.6$ in this example) needs to be used, but this in turn causes the conditioning problem according to Figure 7. Lastly, the RK functions offer the best conditioning in the discrete system, but they converge slightly slower than L-RBFs. This example indicates that L-RBF is the best approach among the tested methods to achieve both exponential convergence and well-conditioned banded discrete system.

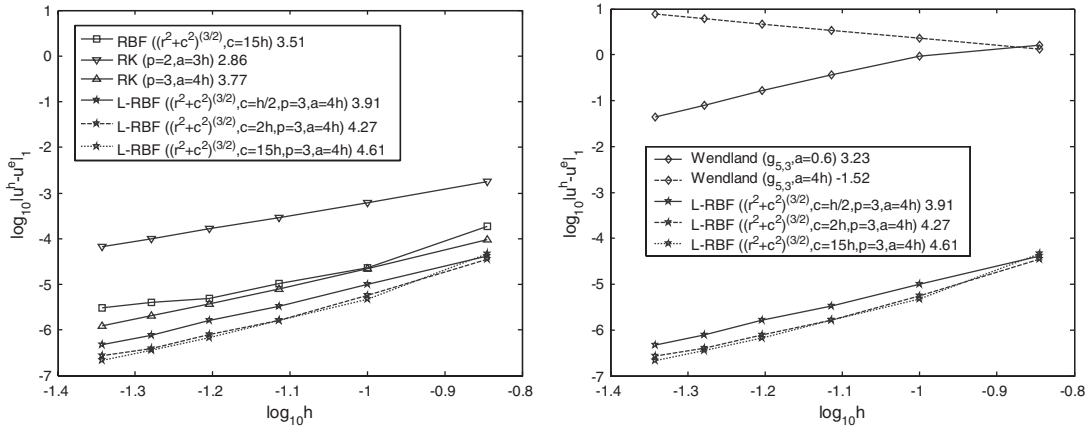


Figure 8. Convergence of H_1 error norm in two-dimensional Poisson problem.

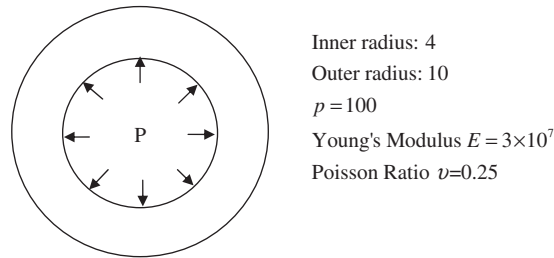


Figure 9. An infinite long cylinder subjected to an internal pressure.

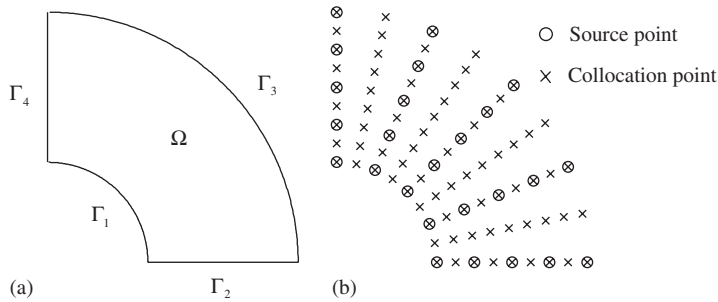


Figure 10. (a) Quarter model and (b) distribution of source and collocation points.

5.3. Elastic cylinder problem

An infinite long elastic cylinder subjected to an internal pressure is shown in Figure 9. Because of symmetry, only a quarter of the model (Figure 10(a)) is considered with proper symmetric boundary conditions imposed. The corresponding boundary value problem can be

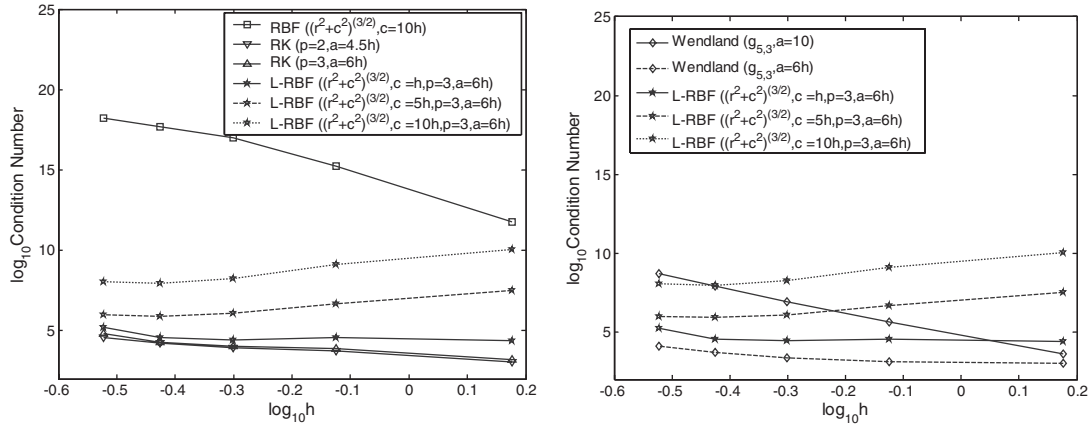


Figure 11. Condition numbers change as refinement in cylinder problem.

expressed as

$$\sigma_{ij,j} = 0 \quad \text{in } \Omega \tag{86}$$

with boundary conditions:

$$\begin{aligned} h_i &= -Pn_i \quad \text{on } \Gamma_1 \\ u_2 = 0, \quad h_1 &= 0 \quad \text{on } \Gamma_2 \\ h_i &= 0 \quad \text{on } \Gamma_3 \\ u_1 = 0, \quad h_2 &= 0 \quad \text{on } \Gamma_4 \end{aligned} \tag{87}$$

where $\sigma_{ij} = C_{ijkl}u_{(k,l)}$ is the stress, C_{ijkl} is the elasticity tensor, u_i is the displacement, $h_i = \sigma_{ijn}j$ is the surface traction, P is pressure, and n_i is the surface normal. The analytical solution to this problem is given as

$$\begin{aligned} u_r(r) &= \frac{Pa^2r}{E(b^2-a^2)} \left[1 - \bar{\nu} + \frac{b^2}{r^2}(1 + \bar{\nu}) \right] \\ u_\theta(r) &= 0 \end{aligned} \tag{88}$$

where $\bar{E} = E/(1 - \nu^2)$, $\bar{\nu} = \nu/(1 - \nu)$, E is Young's modulus, ν is the Poisson ratio, b is the outer radius, and a is the inner radius.

The condition number and convergence in $L2$ and $H1$ error norms are shown in Figures 11–13, respectively. Although Wendland function improves the conditioning of the discrete system compared with that of RBF, the condition number increases as the model is refined when large support is used. The L-RBF approach, on the other hand, yields a very well-conditioned system in all discretizations. Further, L-RBFs offer exceptional convergence rates compared with RK and RBF methods, whereas Wendland functions converge poorly.

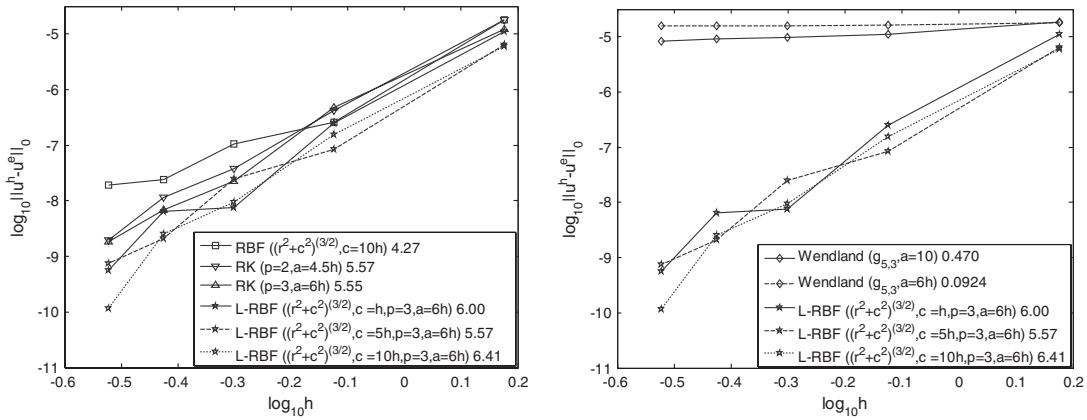


Figure 12. Convergence of \$L_2\$ error norm in cylinder problem.

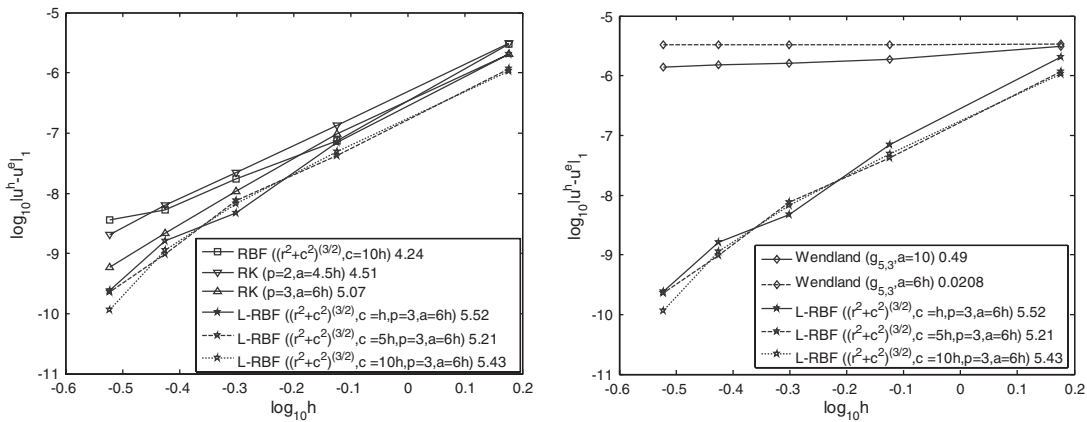


Figure 13. Convergence of \$H_1\$ error norm in cylinder problem.

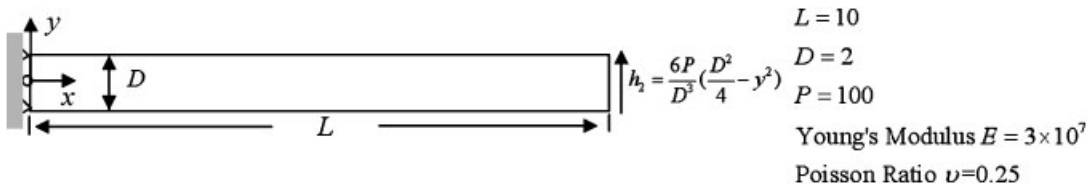


Figure 14. Cantilever problem.

5.4. Cantilever beam problem

Consider a plane-stress elastic cantilever beam subjected to a tip shear traction as shown in Figure 14 with boundary conditions:

$$\begin{aligned} \text{at } x = 0, \quad y = 0, \quad u_1 = u_2 = 0 \\ \text{at } x = 0, \quad y = \pm D/2, \quad u_1 = 0, \quad h_2 = 0 \end{aligned}$$

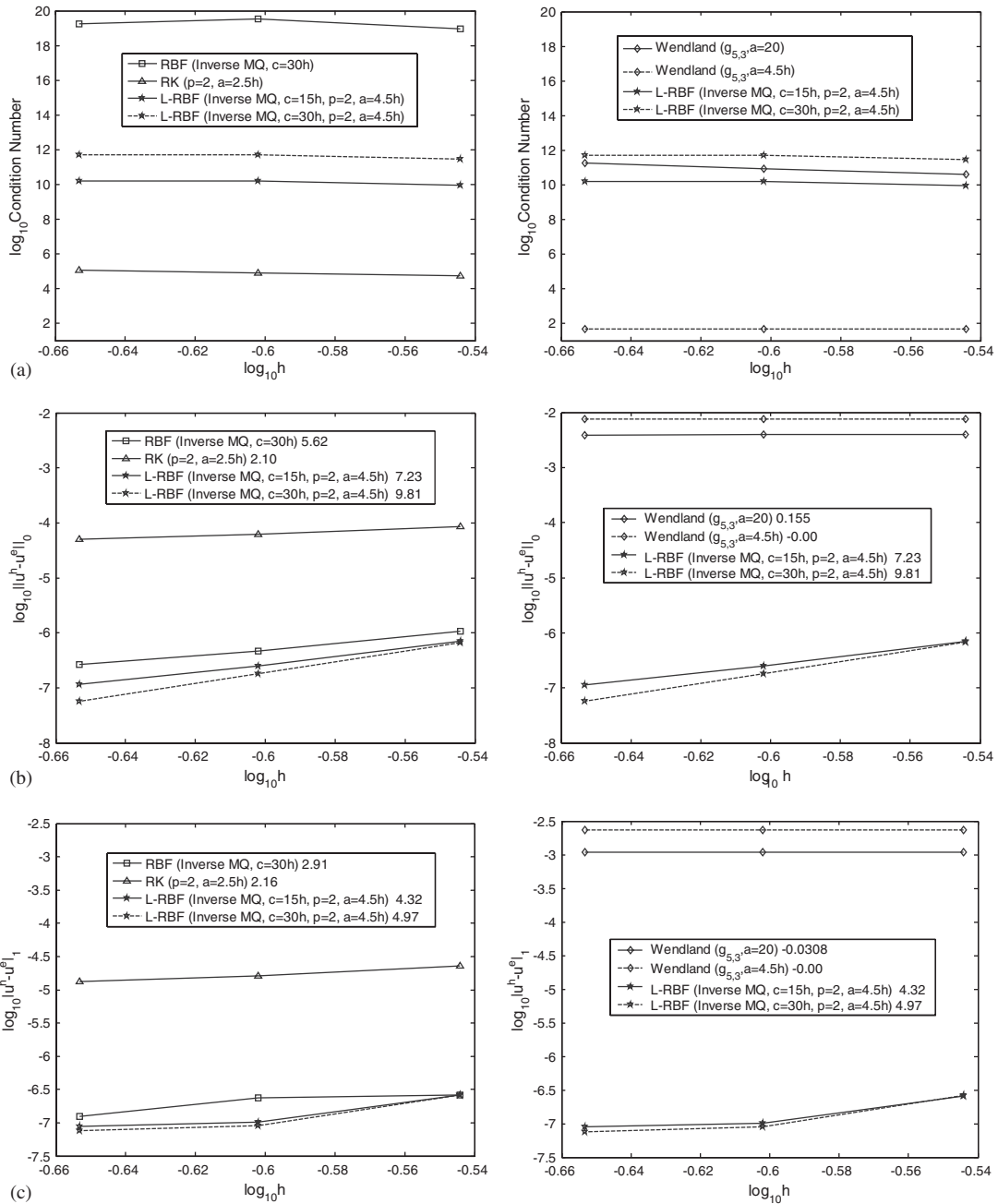


Figure 15. (a) Condition numbers and (b) and (c) convergence of L_2 and H_1 error norm in beam problem.

$$\begin{aligned}
 &\text{on } x = L, \quad -D/2 \leq y \leq D/2, \quad h_1 = 0, \quad h_2 = \frac{6P}{D^3} \left(\frac{D^2}{4} - y^2 \right) \\
 &\text{on } x = 0, \quad -D/2 < y < 0, \quad 0 < y < D/2, \quad h_1 = \frac{12PL}{D^3} y, \quad h_2 = -\frac{6P}{D^3} \left(\frac{D^2}{4} - y^2 \right) \\
 &\text{on } 0 < x < L, \quad y = \pm D/2, \quad H_1 = H_2 = 0
 \end{aligned} \tag{89}$$

where $\sigma_{ij} = C_{ijkl} u_{(k,l)}$ and $h_i = \sigma_{ij} n_j$ as defined in Example 5.3.

The corresponding boundary value problem can be expressed as

$$\sigma_{ij,j} = 0, \quad 0 < x < L, \quad -D/2 < y < D/2 \tag{90}$$

The analytical solution to this problem is given as

$$\begin{aligned}
 u_1(x, y) &= -\frac{Py}{6EI} \left[(6L - 3x)x + (2+n) \left(y^2 - \frac{D^2}{4} \right) \right] \\
 u_2(x, y) &= \frac{P}{6EI} \left[(3L - x)x^2 + 3ny^2(L - x) + (4 + 5n) \frac{D^2 x}{4} \right]
 \end{aligned} \tag{91}$$

where $I = D^3/12$. Four discretizations with 8×36 , 9×41 , and 10×46 source points are used. The collocation points of $(2N_1 - 1) \times (2N_2 - 1)$, where N_i is the number of source points in the i th direction, are employed. The condition number and convergence of L_2 and H_1 error norms are shown in Figure 15(a)–(c). The results show a consistent conclusion of comparison among these methods with the previous example problems. The L-RBF approach yields well-conditioned system and it achieves the best solution accuracy and convergence rates compared with RK function, Wendland function, and standard RBF. It is also shown that the Wendland function yields very poor convergence in this problem.

6. CONCLUSION

The simplicity of RBF collocation method makes it an attractive numerical approach for solving PDEs. The RBFs also offer several appealing features such as the ability to fit through highly irregular scattered data, high-dimensional interpolation, the prewavelet properties for multiresolution analysis with scattered data structure, and the exponential convergence property. Nevertheless, the nature of global approximation in RBFs renders a full matrix and ill-conditioning in the discrete systems. The ill-conditioning is worsened as the discrete model is refined. Thus, RBF approaches are less effective in large-scale computation, in problems involving heterogeneity and small-scale features such as holes and cracks, and in the development of adaptive refinement techniques.

In this work, we formulated a localized RBF (L-RBF) by introducing a reproducing kernel (RK) as the localizing function. The RBF is localized with an RK that possesses polynomial reproducibility. This approach intends to combine the advantages of RBF and RK function to yield a local approximation that is better conditioned than that of RBF, while at the same time offers a higher rate of convergence than that of the RK approximation. The error analysis shows that if the error of RK is sufficiently small, the proposed method maintains the exponential convergence of RBF, while significantly improving the conditioning of the discrete system and yielding a banded matrix.

The numerical tests show that the condition number of the proposed L-RBF is in-between the standard global RBF and the local RK function in coarse discretization. It is observed that the condition numbers increase as discretization is refined in both standard RBF and the Wendland function with large support, whereas the condition numbers in RK and L-RBF are quite insensitive to the resolution of discretization. We observed that for RK and the proposed L-RBF to perform well under collocation method, the employment of sufficiently smooth kernel is essential. In this work, a B-spline kernel with C^5 continuity is used, and the proposed L-RBF achieves about the same level of accuracy and convergence rates as those of the standard RBF. It is noted that the standard RBF solution deteriorates under certain discretization refinement due to ill-conditioning, whereas the L-RBF solution yields a fairly stable convergence as the discretization is refined. It is also shown that for Wendland function to achieve reasonable accuracy and convergence rates, a very large support size is needed. This, however, leads to ill-conditioning as the discretization is refined; similar to that of the standard RBF.

APPENDIX A

The derivation of the inverse inequalities is given as follows. Let v be a function defined in cover (support) ω_I with length $2a_I$ and width $2b_I$. In a two-dimensional setting shown in Figure A1, we denote $\square = \{(\xi, \eta) | -1 \leq \xi \leq 1, -1 \leq \eta \leq 1\}$ and $v(x, y) = v(x(\xi), y(\eta)) = w(\xi, \eta)$. Cover ω_I can be transformed \square into by linear transformation $w = T_I(v)$ and

$$\xi = \frac{1}{a_I}(x - x_I), \quad \eta = \frac{1}{b_I}(y - y_I)$$

Accordingly, it follows that

$$\frac{\partial v}{\partial x} = \frac{\partial w}{\partial \xi} \frac{d\xi}{dx} = \frac{1}{a_I} \frac{\partial w}{\partial \xi}, \quad \frac{\partial v}{\partial y} = \frac{\partial w}{\partial \eta} \frac{d\eta}{dy} = \frac{1}{b_I} \frac{\partial w}{\partial \eta}$$

and

$$dx = a_I d\xi, \quad dy = b_I d\eta$$

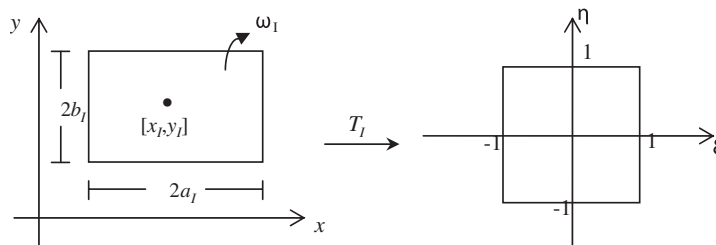


Figure A1. Mapping between physical support to referential support.

We may express any polynomial with a degree of p , $w = w_p = w_p(\xi, \eta) = \sum_{i,j=0}^p b_{ij} \xi^i \eta^j$, by Legendre polynomial, and it possesses the following relationships:

$$\begin{aligned} \left\| \frac{\partial w}{\partial \xi} \right\|_{0,\square} &\leq c_1 p^2 \|w\|_{0,\square}, & \left\| \frac{\partial w}{\partial \eta} \right\|_{0,\square} &\leq c_2 p^2 \|w\|_{0,\square} \\ |w|_{1,\square} &\leq c_3 p^2 \|w\|_{0,\square}, & \|w\|_{1,\square} &\leq c_4 p^2 \|w\|_{0,\square} \end{aligned}$$

For a function v defined in ω_I , we have

$$\begin{aligned} |v|_{1,\omega_I}^2 &= \iint_{\omega_I} (v_x^2 + v_y^2) dx dy = a_I b_I \iint_{\square} \left\{ \left(\frac{1}{a_I} \frac{\partial w}{\partial \xi} \right)^2 + \left(\frac{1}{b_I} \frac{\partial w}{\partial \eta} \right)^2 \right\} d\xi d\eta \\ &= \frac{b_I}{a_I} \iint_{\square} \left(\frac{\partial w}{\partial \xi} \right)^2 d\xi d\eta + \frac{a_I}{b_I} \iint_{\square} \left(\frac{\partial w}{\partial \eta} \right)^2 d\xi d\eta \end{aligned}$$

Correspondingly, we have

$$\begin{aligned} |v|_{1,\omega_I}^2 &= \frac{b_I}{a_I} \left\| \frac{\partial w}{\partial \xi} \right\|_{0,\square}^2 + \frac{a_I}{b_I} \left\| \frac{\partial w}{\partial \eta} \right\|_{0,\square}^2 \leq c_1 \frac{b_I}{a_I} p^4 \|w\|_{0,\square}^2 + c_2 \frac{a_I}{b_I} p^4 \|w\|_{0,\square}^2 \\ &\leq \left(c_1 \frac{b_I}{a_I} + c_2 \frac{a_I}{b_I} \right) p^4 \frac{1}{a_I b_I} \|v\|_{0,\omega_I}^2 \leq \left(c_3 \frac{1}{a_I^2} + c_4 \frac{1}{b_I^2} \right) p^4 \|v\|_{0,\omega_I}^2 \end{aligned}$$

Let $a = \min\{a_I, b_I\}$, the above inequality becomes

$$|v|_{1,\omega_I}^2 \leq c_7 a^{-2} p^4 \|v\|_{0,\omega_I}^2$$

Moreover, we have

$$\|v\|_{1,\omega_I}^2 \leq c_8 a^{-2} p^4 \|v\|_{0,\omega_I}^2$$

Thus, the following result is obtained:

$$\|v\|_{1,\Omega} \leq c \left\{ \sum_{I=1}^N \|v\|_{1,\omega_I}^2 \right\}^{1/2} \leq c\sqrt{\kappa}(a^{-1} p^2) \|v\|_{0,\omega_I} \leq C\sqrt{\kappa}(a^{-1} p^2) \|v\|_{0,\Omega}$$

In general,

$$\begin{aligned} \|v\|_{1,\omega_I} &\leq c_1 a^{-d/2} p^d \|v\|_{0,\omega_I} \\ \|v\|_{1,\Omega} &\leq C_1 \kappa^{1/2} a^{-d/2} p^d \|v\|_{0,\Omega} \end{aligned}$$

and

$$\begin{aligned} \|v\|_{\ell,\omega_I} &\leq c_2 a^{-\ell d/2} p^{\ell d} \|v\|_{0,\omega_I} \quad \text{for } \ell \geq 1 \\ \|v\|_{\ell,\Omega} &\leq C_2 \kappa^{1/2} a^{-\ell d/2} p^{\ell d} \|v\|_{0,\Omega} \quad \text{for } \ell \geq 1 \end{aligned}$$

where d denotes the space dimension.

For the second case, let $v = fg$ be a function defined in cover (support) ω_I with length $2a_I$ and width $2b_I$, and the cover ω_I can be transformed into \square by linear transformation $w = T_I(v)$. Based on the same transformation as above, we have

$$\frac{\partial(fg)}{\partial x} = \frac{\partial f}{\partial x}g + f\frac{\partial g}{\partial x}, \quad \frac{\partial(fg)}{\partial y} = \frac{\partial f}{\partial y}g + f\frac{\partial g}{\partial y}$$

and

$$w_1 = T_I(f), \quad w_2 = T_I(g)$$

Moreover,

$$\begin{aligned} \frac{\partial f}{\partial x} &= \frac{\partial w_1}{\partial \xi} \frac{d\xi}{dx} = \frac{1}{a_I} \frac{\partial w_1}{\partial \xi}, & \frac{\partial f}{\partial y} &= \frac{\partial w_1}{\partial \eta} \frac{d\eta}{dy} = \frac{1}{b_I} \frac{\partial w_1}{\partial \eta} \\ \frac{\partial g}{\partial x} &= \frac{\partial w_2}{\partial \xi} \frac{d\xi}{dx} = \frac{1}{a_I} \frac{\partial w_2}{\partial \xi}, & \frac{\partial g}{\partial y} &= \frac{\partial w_2}{\partial \eta} \frac{d\eta}{dy} = \frac{1}{b_I} \frac{\partial w_2}{\partial \eta} \end{aligned}$$

and

$$\begin{aligned} |v|_{1,\omega_I}^2 &= |fg|_{1,\omega_I}^2 = \iint_{\omega_I} ((fg)_x^2 + (fg)_y^2) dx dy \leq 2 \iint_{\omega_I} ((f_x g)^2 + (f g_x)^2 + (f_y g)^2 + (f g_y)^2) dx dy \\ &= 2a_I b_I \iint_{\square} \left\{ \left(\frac{1}{a_I} \frac{\partial w_1}{\partial \xi} w_2 \right)^2 + \left(\frac{1}{b_I} \frac{\partial w_1}{\partial \eta} w_2 \right)^2 + \left(\frac{1}{a_I} \frac{\partial w_2}{\partial \xi} w_1 \right)^2 + \left(\frac{1}{b_I} \frac{\partial w_2}{\partial \eta} w_1 \right)^2 \right\} d\xi d\eta \end{aligned}$$

There exist the following relationships:

$$\begin{aligned} \left\| \frac{\partial w_1}{\partial \xi} \right\|_{0,\square} &\leq c_1 p^2 \|w_1\|_{0,\square}, & \left\| \frac{\partial w_1}{\partial \eta} \right\|_{0,\square} &\leq c_2 p^2 \|w_1\|_{0,\square}, \\ \left\| \frac{\partial w_2}{\partial \xi} \right\|_{0,\square} &\leq c_3 \mu \|w_2\|_{0,\square}, & \left\| \frac{\partial w_2}{\partial \eta} \right\|_{0,\square} &\leq c_4 \mu \|w_2\|_{0,\square}, \end{aligned}$$

where μ denotes the number of RBFs within cover ω_I . It follows that

$$\begin{aligned} |v|_{1,\omega_I}^2 &= \frac{2b_I}{a_I} \left\| \frac{\partial w_1}{\partial \xi} w_2 \right\|_{0,\square}^2 + \frac{2a_I}{b_I} \left\| \frac{\partial w_1}{\partial \eta} w_2 \right\|_{0,\square}^2 + \frac{2b_I}{a_I} \left\| \frac{\partial w_2}{\partial \xi} w_1 \right\|_{0,\square}^2 + \frac{2a_I}{b_I} \left\| \frac{\partial w_2}{\partial \eta} w_1 \right\|_{0,\square}^2 \\ &\leq \left(c_1 \frac{b_I}{a_I} + c_2 \frac{a_I}{b_I} \right) p^4 \|w_1\|_{0,\square}^2 \|w_2\|_{0,\square}^2 + \left(c_3 \frac{b_I}{a_I} + c_4 \frac{a_I}{b_I} \right) \mu^2 \|w_1\|_{0,\square}^2 \|w_2\|_{0,\square}^2 \\ &\leq \left(c_1 \frac{b_I}{a_I} + c_2 \frac{a_I}{b_I} \right) p^4 \left(\frac{1}{a_I b_I} \right)^2 \|f\|_{0,\omega_I}^2 \|g\|_{0,\omega_I}^2 \end{aligned}$$

$$\begin{aligned}
 & + \left(c_3 \frac{b_I}{a_I} + c_4 \frac{a_I}{b_I} \right) \mu^2 \left(\frac{1}{a_I b_I} \right)^2 \|f\|_{0,\omega_I}^2 \|g\|_{0,\omega_I}^2 \\
 & = \left(c_5 \frac{1}{a_I^3} + c_6 \frac{1}{b_I^3} \right) p^4 \|v\|_{0,\omega_I}^2 + \left(c_7 \frac{1}{a_I^3} + c_8 \frac{1}{b_I^3} \right) \mu^2 \|v\|_{0,\omega_I}^2
 \end{aligned}$$

Let $a = \min\{a_I, b_I\}$, the above inequality becomes

$$|v|_{1,\omega_I}^2 \leq (c_9 a^{-3} p^4 + c_{10} a^{-3} \mu^2) \|v\|_{0,\omega_I}^2$$

Moreover, we have

$$\|v\|_{1,\omega_I}^2 \leq (c_{11} a^{-3} p^4 + c_{12} a^{-3} \mu^2) \|v\|_{0,\omega_I}^2$$

Consequently, the following result is obtained:

$$\|v\|_{1,\Omega} \leq c\sqrt{\kappa}(c_1 a^{-3/2} p^2 + c_2 a^{-3/2} \mu) \|v\|_{0,\omega_I} \leq C\sqrt{\kappa}(c_1 a^{-3/2} p^2 + c_2 a^{-3/2} \mu) \|v\|_{0,\Omega}$$

In d -dimensional space, we have

$$\begin{aligned}
 \|v\|_{1,\omega_I} & \leq (c_1 a^{-3d/4} p^d + c_2 a^{-3d/4} \mu^{d/2}) \|v\|_{0,\omega_I} \\
 \|v\|_{1,\Omega} & \leq (C_1 \kappa^{1/2} a^{-3d/4} p^d + C_2 \kappa^{1/2} a^{-3d/4} \mu^{d/2}) \|v\|_{0,\Omega}
 \end{aligned}$$

and

$$\begin{aligned}
 \|v\|_{\ell,\omega_I} & \leq (c_1 a^{-3\ell d/4} p^{\ell d} + c_2 a^{-3\ell d/4} \mu^{\ell d/2}) \|v\|_{0,\omega_I} \quad \text{for } \ell \geq 1 \\
 \|v\|_{\ell,\Omega} & \leq (C_1 \kappa^{1/2} a^{-3\ell d/4} p^{\ell d} + C_2 \kappa^{1/2} a^{-3\ell d/4} \mu^{\ell d/2}) \|v\|_{0,\Omega} \quad \text{for } \ell \geq 1
 \end{aligned}$$

where c_i and C_i are generic constants. For the case of elliptic and circular covers, similar results can be obtained.

ACKNOWLEDGEMENTS

The support of this work by Lawrence Livermore National Laboratory (USA) to the first and second authors and the support by National Science Council (Taiwan, Republic of China) to the third author are greatly acknowledged.

REFERENCES

1. Hardy RL. Multiquadric equations of topography and other irregular surfaces. *Journal of Geophysics Research* 1971; **176**:1905–1915.
2. Hardy RL. Theory and applications of the multiquadric-biharmonic method: 20 years of discovery. *Computers and Mathematics with Applications* 1990; **19**(8/9):163–208.
3. Carlson RE, Foley TA. Interpolation of track data with radial basis methods. *Computers and Mathematics with Applications* 1992; **24**:27–34.
4. Girosi F. On some extensions of radial basis functions and their applications in artificial intelligence. *Computers and Mathematics with Applications* 1992; **24**:61–80.
5. Buhmann MD, Micchelli CA. Multiquadric interpolation improved advanced in the theory and applications of radial basis functions. *Computers and Mathematics with Applications* 1992; **43**:12, 21–25.

6. Chui CK, Stoeckler J, Ward JD. Analytic wavelets generated by radial functions. *Advances in Computational Mathematics* 1996; **5**:95–123.
7. Kansa EJ. Multiquadrics—a scattered data approximation scheme with applications to computational fluid-dynamics—I. Surface approximations and partial derivatives. *Computers and Mathematics with Applications* 1992; **19**:127–145.
8. Kansa EJ. Multiquadrics—a scattered data approximation scheme with applications to computational fluid-dynamics—II. Solutions to parabolic, hyperbolic and elliptic partial differential equations. *Computers and Mathematics with Applications* 1992; **19**:147–161.
9. Franke R, Schaback R. Solving partial differential equations by collocation using radial functions. *Applied Mathematics and Computation* 1998; **93**:73–82.
10. Wendland H. Meshless Galerkin methods using radial basis functions. *Mathematics of Computation* 1999; **68**(228):1521–1531.
11. Hu HY, Li ZC, Cheng AHD. Radial basis collocation method for elliptic equations. *Computers and Mathematics with Applications* 2005; **50**:289–320.
12. Cecil T, Qian J, Osher S. Numerical methods for high dimensional Hamilton–Jacobi equations using radial basis functions. *Journal of Computational Physics* 2004; **196**:327–347.
13. Li J. Mixed methods for fourth-order elliptic and parabolic problems using radial basis functions. *Advances in Computational Mathematics* 2005; **23**:21–30.
14. Pollandt R. Solving nonlinear equations of mechanics with the boundary element method and radial basis functions. *International Journal for Numerical Methods in Engineering* 1997; **40**:61–73.
15. Sonar T. Optimal recovery using thin-plate splines in finite volume methods for the numerical solution of hyperbolic conservation laws. *IMA Journal of Numerical Analysis* 1996; **16**:549–581.
16. Fasshauer GE. Solving differential equations with radial basis functions: multilevel methods and smoothing. *Advances in Computational Mathematics* 1999; **11**:139–159.
17. Hu HY, Chen JS, Hu W. Weighted radial basis collection method for boundary value problems. *International Journal for Numerical Methods in Engineering* 2001; **69**:2736–2757.
18. Madych WR, Nelson SA. Bounds on multivariate polynomials and exponential error estimates for multiquadric interpolation. *Journal of Approximation Theory* 1992; **70**:94–114.
19. Madych WR, Nelson SA. Multivariate interpolation and conditionally positive definite functions. II. *Mathematics of Computation* 1990; **54**(189):211–230.
20. Hon YC, Schaback R. On unsymmetric collocation by radial basis functions. *Applied Mathematics and Computation* 2001; **119**:177–186.
21. Kansa EJ, Hon YC. Circumventing the ill-conditioning problem with multiquadric radial basis functions: applications to elliptic partial differential equations. *Computers and Mathematics with Applications* 2000; **4**:123–137.
22. Wong SM, Hon YC, Li TS, Chung SL, Kansa EJ. Multizone decomposition for simulation of time-dependent problems using the multiquadric scheme. *Computers and Mathematics with Applications* 1999; **37**:23–43.
23. Ling L, Opfer R, Schaback R. Results on meshless collocation techniques. *Engineering Analysis with Boundary Elements* 2006; **30**:247–253.
24. Wendland H. Piecewise polynomial, positive definite and compactly supported radial basis functions of minimal degree. *Advances in Computational Mathematics* 1995; **4**:389–396.
25. Belytschko T, Lu YY, Gu L. Element-free Galerkin methods. *International Journal for Numerical Methods in Engineering* 1994; **37**:229–256.
26. Lancaster P, Salkauskas K. Surfaces generated by moving least squares methods. *Mathematics of Computation* 1981; **37**:141–158.
27. Chen JS, Pan C, Wu CT, Liu WK. Reproducing kernel particle methods for large deformation analysis of nonlinear structures. *Computer Methods in Applied Mechanics and Engineering* 1996; **139**:195–227.
28. Liu WK, Jun S, Zhang YF. Reproducing kernel particle methods. *International Journal for Numerical Methods in Fluids* 1995; **20**:1081–1106.
29. Babuska I, Melenk JM. The partition of unity method. *International Journal for Numerical Methods in Engineering* 1997; **40**:727–758.
30. Duarte CAM, Oden JT. *Hp* clouds—an *hp* meshless method. *Numerical Methods for Partial Differential Equations* 1996; **12**:673–705.
31. Chen JS, Wu CT, Yoon S, You Y. A stabilized conforming nodal integration for Galerkin meshfree methods. *International Journal for Numerical Methods in Engineering* 2001; **50**:435–466.

32. Chen JS, Wu CT, Yoon S, You Y. Nonlinear version of stabilized conforming nodal integration for Galerkin meshfree methods. *International Journal for Numerical Methods in Engineering* 2002; **53**:2587–2615.
33. Chen JS, Wang HP. New boundary condition treatments in meshless computation of contact problems. *Computer Methods in Applied Mechanics and Engineering* 2000; **187**:441–468.
34. Huerta A, Fernández-Méndez S. Enrichment and coupling of the finite element and meshless methods. *International Journal for Numerical Methods in Engineering* 2000; **48**:1615–1636.
35. Madych WR. Miscellaneous error bounds for multiquadric and related interpolatory. *Computers and Mathematics with Applications* 1992; **24**(12):121–138.
36. Buhmann MD. *Radial Basis Functions*. Cambridge University Press: Cambridge, 2003.
37. Golomb M, Weinberger HF. *Optimal Approximation and Error Bounds on Numerical Approximation*. University of Wisconsin Press: Madison, 1959.
38. Cheng AH-D, Golberg MA, Kansa EJ, Zammito G. Exponential convergence and H-c multiquadrics collection method for partial differential equations. *Numerical Methods for Partial Differential Equations* 2003; **19**:571–594.
39. Han W, Meng X. Error analysis of the reproducing kernel particle method. *Computer Methods in Applied Mechanics and Engineering* 2001; **190**:6157–6181.